LAMINAR EDDIES IN A TWO-DIMENSIONAL CONDUIT EXPANSION

BY TIN-KAN HUNG * AND ENZO O. MACAGNO **

Introduction

As is well known, very few solutions of laminar flow implying complete forms of the Navier-Stokes equations have been obtained analytically; most of the known solutions of laminar flows are based on simplified equations. With the advent of the modern electronic computers it has become possible to calculate laminar flows using discretized forms of the fundamental equations of viscous-fluid flow [1, 2]; certain finite-difference forms of these equations have been known for some decades and were integrated in a few cases using desk calculators [3]. In this paper, the results of calculations performed with an electronic computer for the zone of separation in a two-dimensional conduit expansion of ratio 2:1 are presented; flow patterns and vorticity contours are given for Reynolds numbers from zero to 333. Two methods were used, one involving the direct determination of the steady-state solution from equations without unsteady terms, and the other based on approaching the solution asymptotically by numerical integration of the equations with local acceleration terms. For equal conditions, the unsteady approach showed computational stability when the steady approach became unstable; when both methods were stable, the results agreed very well.

* Research Associate, Institute of Hydraulic Research, The University of Iowa, Iowa City, Iowa.

** Associate Professor, Department of Mechanics and Hydraulics; Research Engineer, Institute of Hydraulic Research, The University of Iowa, Iowa City, Iowa.

Fundamental equations

There is experimental evidence of symmetric and stable laminar flow in conduit expansions [4, 5] for relatively low Reynolds numbers, and on this basis the flow in a two-dimensional conduit with a sudden expansion (Fig. 1) was assumed to be symmetric, and steady-state solutions were investigated. The Navier-Stokes equations for two-dimensional flow in terms of the cartesian coordinates x and y are

$$u_t + uu_x + vu_y = -p_x + \frac{1}{\mathcal{R}}(u_{xx} + u_{yy}) \quad (1)$$

$$v_t + uv_x + vv_y = -p_y + \frac{1}{\mathcal{R}}(v_{xx} + v_{yy}) \quad (2)$$

Herein, u and v represent the velocity components in the x and y directions, respectively; the x-axis has been taken along the lower wall of the wider part of the conduit. The two equations are

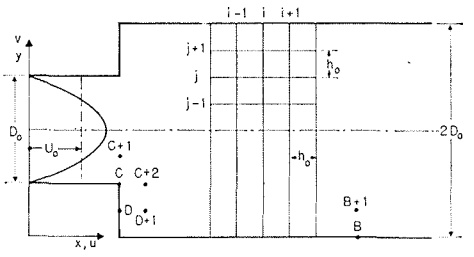

1/ Definition sketch.
Croquis de définition.

dimensionless with reference to the spacing D_0 and the average velocity U_0 (Fig. 1); i.e., p indicates the ratio of the pressure to the quantity ρU_0^2 (ρ is the density of the fluid), while x, y, and t are referred, respectively, to D_0, and to D_0/U_0. The Reynolds number is given by $\mathcal{R} = U_0 D_0/\nu$, where ν is the kinematic viscosity. Subscripts are used to indicate partial derivatives. To the two preceding equations, the equation of continuity

$$u_x + v_y = 0 \tag{3}$$

must be added.

Upon the elimination of the pressure between Eqs. (1) and (2) and introduction of the vorticity

$$\zeta = v_x - u_y \tag{4}$$

the following expression is obtained

$$\zeta_t + u\zeta_x + v\zeta_y = \frac{1}{\mathcal{R}} (\zeta_{xx} + \zeta_{yy}) \tag{5}$$

If the expressions are introduced for the velocity components in terms of the derivatives of the stream function ψ,

$$u = \psi_y \qquad v = -\psi_x \tag{6}$$

the equations

$$\zeta = -\psi_{xx} - \psi_{yy} \tag{7}$$

$$\zeta_t + \psi_y\zeta_x - \psi_x\zeta_y = \frac{1}{\mathcal{R}} (\zeta_{xx} + \zeta_{yy}) \tag{8}$$

result from Eqs. (4) and (5), respectively. Substitution of the first of these last two equations into the second would result in a single fourth-order differential equation for the stream function. Past experience [3] with such an equation has indicated serious difficulties; therefore, it was decided to work with Eqs. (7) and (8), which are known to provide a more tractable system from which both the vorticity and the stream function are determined simultaneously.

Two different approaches were followed in the investigation of the flow in the conduit expansion. One, which will be called the steady approach, consisted in calculating the steady-state solution using Eq. (8) without the unsteady term ζ_t; the other, called the unsteady approach, was based on applying Eq. (8), as it stands, to one of the solutions already obtained by the steady approach. The unsteady approach made it possible to pass, without changing mesh size, from the flow at one Reynolds number to the flow at a substantially higher (or lower) Reynolds number.

The difference equations for the steady approach [3] are

$$\psi_{i,j}^{k+1} = \frac{1}{4} \left(\psi_{i-1,j}^{k+1} + \psi_{i,j-1}^{k+1} + \psi_{i,j+1}^{k} + \psi_{i+1,j}^{k} + h^2 \zeta_{i,j}^{k+1} \right) \tag{9}$$

$$\zeta_{i,j}^{k+1} = \frac{1}{4} (\zeta_{i-1,j}^{k+1} + \zeta_{i,j-1}^{k+1} + \zeta_{i,j+1}^{k} + \zeta_{i+1,j}^{k}) + \frac{\mathcal{R}}{16} \left[\begin{array}{l} (\psi_{i+1,j}^{k} - \psi_{i-1,j}^{k}) (\zeta_{i,j+1}^{k} - \zeta_{i,j-1}^{k+1}) \\ - (\psi_{i,j+1}^{k} - \psi_{i,j-1}^{k}) (\zeta_{i+1,j}^{k} - \zeta_{i-1,j}^{k+1}) \end{array} \right] \tag{10}$$

These equations are obtained from Eqs. (7) and (8) for $\zeta_t = 0$, using the following three-point central-difference formula for the first derivative in the x-direction

$$(\zeta_x)_{i,j} = \frac{1}{2h} (\zeta_{i+1,j} - \zeta_{i-1,j}) - \frac{h^2}{6} \zeta_{xxx}(x_1, y) \tag{11}$$

Herein x_1 satisfies the expression

$$x - h < x_1 < x + h$$

Entirely similar formulas were used for the ζ_y, and for the function ψ. If the dimensionless mesh size h is relatively small (i.e., h_0/D_0 small), the error term in the right-hand side can be neglected. The finite-difference formula used for the Laplacian of the vorticity was

$$(\zeta_{xx} + \zeta_{yy})_{i,j} = \frac{1}{h^2} \times \times (\zeta_{i-1,j} + \zeta_{i,j-1} + \zeta_{i,j+1} + \zeta_{i+1,j} - 4\zeta_{i,j}) \tag{12}$$

In the finite-difference equations (9) and (10), the index k indicates the number of iterations; these are performed in the directions of increasing j and i, or, what is equivalent, in the direction of increasing y and x.

For the unsteady approach the difference equations [1] are the following :

$$\zeta_{i,j}^{n+1} = \left(\frac{4}{h^2} + \frac{\mathcal{R}}{2\,\delta t} \right)^{-1} \times \left\{ \begin{array}{l} \dfrac{\mathcal{R}}{2\,\delta t} \zeta_{i,j}^{n-1} \\ + \dfrac{1}{h^2} (\zeta_{i+1,j}^{n} + \zeta_{i-1,j}^{n} + \zeta_{i,j+1}^{n} + \zeta_{i,j-1}^{n}) \\ + \dfrac{\mathcal{R}}{4h^2} \left[\begin{array}{l} (\psi_{i+1,j}^{n} - \psi_{i-1,j}^{n}) (\zeta_{i,j+1}^{n} - \zeta_{i,j-1}^{n}) \\ - (\psi_{i,j+1}^{n} - \psi_{i,j-1}^{n}) (\zeta_{i+1,j}^{n} - \zeta_{i-1,j}^{n}) \end{array} \right] \end{array} \right\} \tag{13}$$

$$\psi_{i,j}^{n+1} = \frac{1}{4} \left(\psi_{i-1,j}^{n+1} + \psi_{i,j-1}^{n+1} + \psi_{i,j+1}^{n+1} + \psi_{i+1,j}^{n+1} + h^2 \zeta_{i,j}^{n+1} \right) \tag{14}$$

Herein n represents the time index. It should be noted that the first of these two equations indicates that ζ at the time $(n+1)\,\delta t$ can be calculated from the settled values of ψ and ζ at the time $n\delta t$, and ζ at $(n-1)\,\delta t$. After computations of ζ at the time $(n+1)\,\delta t$ are completed, Eq. (14) is used to calculate the stream function by iteration.

Steady approach

Because it seemed so obvious that steady-state solutions would be more easily obtained from equations without unsteady terms, the first part of this investigation was devoted to the integration of Eqs. (9) and (10) starting from the limiting case of vanishing inertia forces; this is the well-known case of creeping flow. Once the flow was known

for a given Reynolds number, this number was increased in the Eq. (10) and the calculation was repeated until settled values were obtained again. For a given mesh size, due to computational instability, this process can be continued successfully only up to a certain Reynolds number; it then becomes necessary to use a mesh of smaller size. The influence of mesh size and ways of sweeping the field on the stability of the calculations were investigated by means of a disturbed uniform flow, for which calculations were performed upon a portion of the two-dimensional conduit. The results of this particular investigation, in which the exact vorticity distribution was first disturbed and then recalculated numerically, will be reported elsewhere [6].

Due to the use of equations for the stream function and the vorticity, instead of the stream function alone, the boundary conditions need more complex expressions than the simple specification of the non-slip condition on fixed walls :

$$u = \psi_y = 0 \qquad v = -\psi_x = 0 \qquad (15)$$

Because only symmetrical flows are contemplated, the value of the stream function on the center line must be assumed to be constant. On the center line the velocity component in the y-direction $v = -\psi_x$ is zero, but not the u-component.

The conditions for the vorticity on the walls will now be specified. For a wall parallel to the x-axis, the expansion of ψ about the point B on the boundary gives

$$\psi_{B+1} = \psi_B + h\,(\psi_y)_B + \frac{h^2}{2!}\,(\psi_{yy})_B + \frac{h^3}{3!}\,(\psi_{yyy})_B + \frac{h^4}{4!}\,(\psi_{yyyy})_B + O\,(h^5) \qquad (16)$$

If one takes into account that ψ_y, ψ_{xx}, ψ_{xxy}, and ψ_{xxxx} are all zero on the fixed boundary, the following expressions can be found

$$(\psi_{yy})_B = -\zeta_B$$
$$(\psi_{yyy})_B = -(\zeta_y)_B$$
$$(\psi_{yyyy})_B = (\zeta_{xx})_B - (\zeta_{yy})_B$$

Substitution of the preceding expressions into Eq. (16) gives

$$\psi_{B+1} = \psi_B - \frac{h^2}{2!}\,\zeta_B - \frac{h^3}{3!}\,(\zeta_y)_B + \frac{h^4}{4!}\,(\zeta_{xx} - \zeta_{yy})_B + O\,(h^5) \qquad (17)$$

From an expansion of ζ about B, the following expression results :

$$(\zeta_y)_B = \frac{1}{h}\,(\zeta_{B+1} - \zeta_B) - \frac{h}{2}\,(\zeta_{yy})_B + O\,(h^2) \qquad (18)$$

From Eqs. (17) and (18) the vorticity at B + 1 is obtained [7] as

$$\zeta_B = \frac{3}{h^2}\,(\psi_B - \psi_{B+1}) - \frac{1}{2}\,\zeta_{B+1} + \frac{h^2}{8}\,(\zeta_{xx} + \zeta_{yy}) + O\,(h^3) \qquad (19)$$

On the boundary, $\zeta_t = 0$; therefore,

$$\zeta_B = \frac{3}{h^2}\,(\psi_B - \psi_{B+1}) - \frac{1}{2}\,\zeta_{B+1} + O\,(h^3) \qquad (20)$$

In a similar manner, for a wall parallel to the y-axis, the following expression can be derived for the vorticity :

$$\zeta_D = \frac{3}{h^2}\,(\psi_D - \psi_{D+1}) - \frac{1}{2}\,\zeta_{D+1} + O\,(h^3) \qquad (21)$$

For the point C, Eq. (20) was used, because separation makes the flow there nearly parallel to the x-axis. Another formula, in which values at points C + 1 and C + 2 were considered, was tested, but it did not yield as good results as Eq. (21) for the local values of the vorticity. However, the difference in the shape and the size of the eddies was practically negligible.

Obviously, for a computational solution, the length of conduit must be as short as compatible with the desired accuracy. The inlet section was located at a distance from the expansion that provided a short portion of flow that was very nearly uniform; it was found that a distance as small as $3\,D_0/4$ could be used for this purpose. The downstream end of the flow was given more careful consideration, because conditions on this side were expected to have a stronger influence on the eddy size and configuration. Variation of the distance from the expansion to the outlet was sufficient to indicate beyond doubt the length necessary to obtain eddy characteristics that would remain unaffected by further displacement downstream of the outlet section. It was found that the parabolic velocity distribution could be imposed as near as D_0 from the reattachment point without appreciable effect on the eddy zone. Furthermore, the specification of kinematic conditions at the outlet was also the object of computational experimentation; instead of imposing the parabolic velocity distribution at the outlet, a more flexible condition was prescribed based on Milne's predictor formula [8] and formula (11). The following expressions were thus used for the stream function and the vorticity :

$$\psi_{i,j} = \psi_{i-4,j} - 2\,\psi_{i-3,j} + 2\,\psi_{i-1,j} \qquad (22)$$

$$\zeta_{i,j} = \zeta_{i-4,j} - 2\,\zeta_{i-3,j} + 2\,\zeta_{i-1,j} \qquad (23)$$

Herein i is the index for the x-coordinate at the outlet. These formulas only project the trend resulting from upstream, and the result is adopted as valid for the next iteration. This second treatment was used for $\mathcal{R} = 0$ and $\mathcal{R} = 48$ and was checked against results obtained by other means. Because the treatment was found computationally satisfactory and provided a more plausible flow condition at the outlet, it was also used in the unsteady approach.

To determine the two functions ψ and ζ, one should do the following :

1) Start from an assumed distribution of ψ and ζ, for a given flow condition, or, preferably, use the results of a previous solution for a lower Reynolds number.
2) Calculate ζ^{k+1} using Eq. (10), for all inner points of the field.

Table 1

D_o/h_o	R	e	k \ y/D_o	4/8	5/8	6/8	7/8	1
8	40	0.5	125	0	0.042957	0.156246	0.316407	0.500000
16	40	0.2	75	0	0.042968	0.156250	0.316406	0.500000
16	40	1	75	0	0.042968	0.156250	0.316406	0.500000
32	80	0.5	30	0	0.042924	0.156152	0.316328	0.500000
Exact values of ψ				0	0.042968	0.156250	0.316406	0.500000
D_o/h_o	R	e	k \ y/D_o	4/8	5/8	6/8	7/8	1
8	40	0.5	125	— 5.995450	— 5.048380	— 3.010947	— 1.521108	0
16	40	0.2	75	— 5.999999	— 4.499999	— 2.999999	— 1.499999	0
16	40	1	75	— 5.999999	— 4.499999	— 2.999999	— 1.499999	0
32	80	0.5	30	— 5.994160	— 4.495195	— 2.999685	— 1.500543	0
Exact values of ζ				— 6.000000	— 4.500000	— 3.000000	— 1.500000	0

Verification of the computational scheme by calculating Poiseuille flow starting from an initial distribution of vorticity disturbed by alternately applied factors $(1 \pm e)$. D_o/h_o is the number of meshes, R is the Reynolds number, k is the number of iterations.

3) Compute ψ^{k+1} by Eq. (9) for all inner points.

4) If the second treatment is used for the outlet, apply Eqs. (22) and (23) to calculate ψ^{k+1} and ζ^{k+1}. Calculate ζ^{k+1} on the wall using Eq. (20) or Eq. (21).

5) Repeat steps 2 to 4 until the two functions are settled.

As shown by the iteration index in Eqs. (9) and (10), the method adopted consists in utilizing available projected values of the stream function and the vorticity during the iteration. This accelerates the iteration process and saves computer storage and time.

Experience shows that after a number of iterations a stable computation leads to a stabilized realistic flow pattern. However, calculations with the above-mentioned disturbed uniform flow have shown that the settled values may differ from the exact solution known for this flow. Fortunately, the deviations found for the present calculations were very small, as shown in Table 1, and it was assumed that they would remain small also for the non-uniform flow. The following two conditions were selected for the numerically calculated functions ψ and ζ :

$$\frac{|\psi_{i,j}^{k+10} - \psi_{i,j}^{k}|}{\psi_0} \leqslant 0.000015 \qquad (24)$$

$$\frac{|\zeta_{i,j}^{k+10} - \zeta_{i,j}^{k}|}{\zeta_0} \leqslant 0.0001 \qquad (25)$$

Herein ψ_0 is the dimensionless discharge, and ζ_0 is the wall vorticity at the inlet. It was assumed that the flow had reached its final configuration when the conditions expressed by Eqs. (24) and (25) were satisfied. These conditions are more than is really needed for the sole determination of streamlines; they were adopted in order to have an approximation that would permit eventual calculation of pressure and velocity, normal and tangential viscous stresses, and terms of the momentum and energy equations [9].

Unsteady approach

In any actual experiment with the purpose of determining a zone of separation the fluid must be accelerated gradually from a state of rest. In other words, one would not think of instantaneously producing the desired steady flow. It seems, after this, that a more natural computational scheme to determine the zone of separation should be one that duplicates computationally what is done physically. This was done, however, only after unsurmountable difficulties were encountered in the steady approach, which at the beginning was believed to be simpler and less time-consuming. In fact, the unsteady approach proved to be as easy to handle as the steady approach and much more stable. The steady approach provided a different way of obtaining flow patterns and served as a check as well as a guide for the unsteady approach, but the latter approach should be recommended for any new investigation. The procedure used was the change of the Reynolds number in the Eq. (13) without changing stream-function values on the boundaries, which can be considered as a sudden change in viscosity while keeping the discharge constant. The uniform-flow condition at the computational inlet was not changed either.

For the unsteady approach, the boundary conditions for the stream function are not different from the ones used in the steady approach, but the conditions for the vorticity at the walls should be changed. An attempt to use appropriate forms of these conditions in the form of explicit time-dependent expressions of the boundary vorticity led to numerical instability. It was then decided to use Eqs. (20) and (21), which can be considered as an approximation of the actual conditions, because the term neglected $[(h^2/8)\ \nabla^2\zeta_B]$ is small; it should be noted that these expressions do not neglect completely the variation of vorticity with time, because the inner values used in them are taken at the correct time. Results of this technique for certain Reynolds numbers could be checked, because steady-approach solutions had already been obtained; the comparison showed a very satisfactory agreement. It is presumed that solutions for higher Reynolds numbers would have equally good agreement, because the unsteady terms after a large number of time steps become very small, and one is actually calculating with a quasi-steady approach, the unsteady terms helping to keep the computational model stable but with almost no influence on the results. When the values of ψ and ζ, thus determined for $\mathcal{R} = 333$, were introduced in the equations for the steady approach (for the same Reynolds number), computational instability arose almost immediately.

The calculation instructions for the unsteady approach were the following :

1) Feed the computer with the data for an initial known solution for a certain Reynolds number $\mathcal{R}_1$. Change the Reynolds number into $\mathcal{R}_2$ without modifying the values of ψ and ζ.
2) Calculate ζ^{n+1} in all interior points using Eq. (13), and at the outlet with Eq. (23).
3) Obtain new values of ψ applying an iteration process in which new values of ζ at the time $(n+1)\ \delta t$ are used. In this step, Eq. (14) is used over the inner field and Eq. (22) at the computational outlet.
4) Calculate vorticity on the wall by Eqs. (20) and (21).
5) Repeat steps (2) and (4) until the control for the time variable terminates it.

In order to save computer time, a less-stringent requirement than for the preceding calculations for the steady approach was used to determine when the flow could be considered settled :

$$\frac{|\psi_{i,j}^{k+10} - \psi_{i,j}^{k}|}{\psi_0} \leqslant 0{,}0003 \qquad (26)$$

In addition, only that part of the field that showed more sensitivity to time-variation disturbances was subject to this control. This critical region was found computationally to be in the neighborhood of the reattachment point. Observations of the laminar eddy in a small flume also showed fluctuations in the reattachment-point region, while the rest of the flow was apparently steady.

The stability criteria indicated by J. E. Fromm [1] were used; rewritten in terms of the dimensionless quantities h, u, t, and $\mathcal{R}$, they are

$$\frac{u\delta t}{h} < 1 \qquad \text{and} \qquad \frac{\delta t}{\mathcal{R}h^2} < \frac{1}{4}$$

Two different time increments (0.0133 and 0.02) were used, and they gave practically no difference in the flow patterns. To investigate the possibility of reducing storage in the computer, the flow pattern for $\mathcal{R} = 333$ was also determined with a rectangular mesh of ratio $\delta x/\delta y = 2$. No appreciable difference was found, and it was concluded that for long eddies the use of rectangular meshes offers definite advantages.

Computational results

A series of flow patterns and their corresponding vorticity contours, as obtained with the steady approach, are shown in Figures 2 and 3. These figures represent only a part of the calculations that covered the range of Reynolds numbers from 0 up to nearly 100. The results for 16 and 32 were obtained using a mesh size of 1/16, while the results for all other Reynolds numbers in Figures 2 and 3 correspond to calculations with a finer mesh of 1/32. The values on streamlines and on vorticity contour lines given in these figures, for 16 and 48, apply to the other Reynolds numbers as well, unless otherwise indicated.

The calculations were started for $\mathcal{R} = 0$, for which an approximate flow pattern was first drawn by hand without flow separation, values for the stream function were then read out from this flow pattern and used as the first set for a series of iterations. A small eddy in the corner resulted for $\mathcal{R} = 0$, and, because there were some doubts about its actual existence, a calculation for a very low Reynolds number of 0.2 was then carried out; in these calculations, the inertia terms were present and not neglected as in the preceding case, a factor that should ensure a more realistic solution; practically the same size of eddy with a slightly larger intensity of flow was obtained. Hence, it was assumed that the eddy for $\mathcal{R} = 0$ was not merely due to the calculational procedure. A word of explanation is perhaps warranted in connection with the "flow" for $\mathcal{R} = 0$; it should be understood that one refers to a creeping flow for which the inertia terms are considered to be vanishingly small. If the Reynolds number is considered as a multiplier of those terms, instead of a divider of the viscous terms as is usually presented, and as tending to zero because of an ever increasing viscosity, it becomes clear that the terms left are the viscous terms as part of a biharmonic equation, the solution of which is characterized by $\mathcal{R} = 0$.

In Figures 2 and 3 it can be seen that the laminar eddy becomes longer as the Reynolds number increases; the vorticity contour lines are stretched downstream by convection effects while the diffusion effects become smaller. The maximum vorticity values are not on the line of separation, but on the main flow; they gradually come back to the wall downstream from the reattachment point, which is a point of zero vorticity.

Results of calculations using the unsteady approach are shown in Figure 4, in which the flow

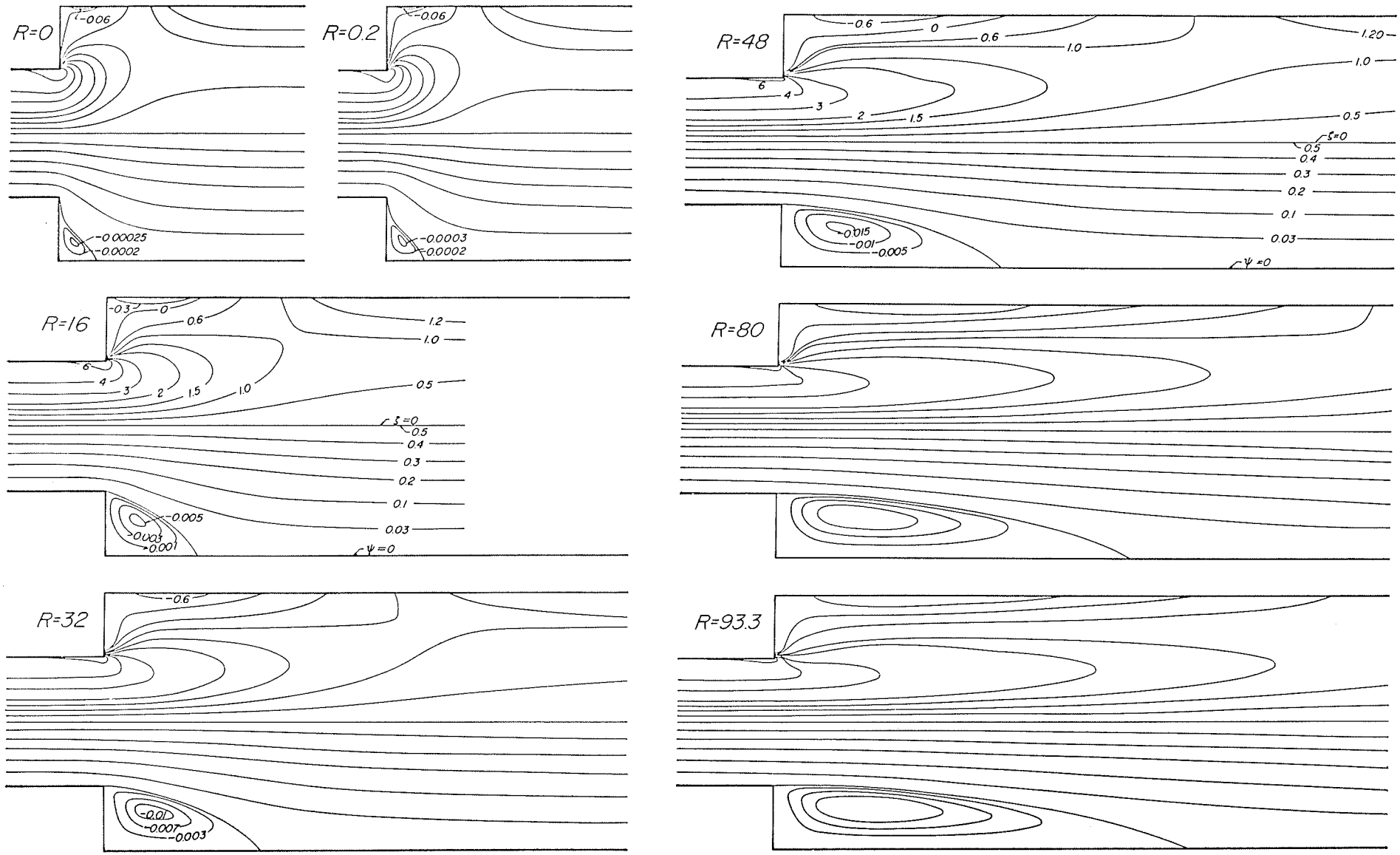

2/ et 3/ Vorticity contour lines and streamlines for steady laminar flow in a two-dimensional conduit expansion.

Profils de vorticité et répartition des lignes de courant correspondant à un écoulement plan par un élargissement de conduite, en régime permanent et laminaire.

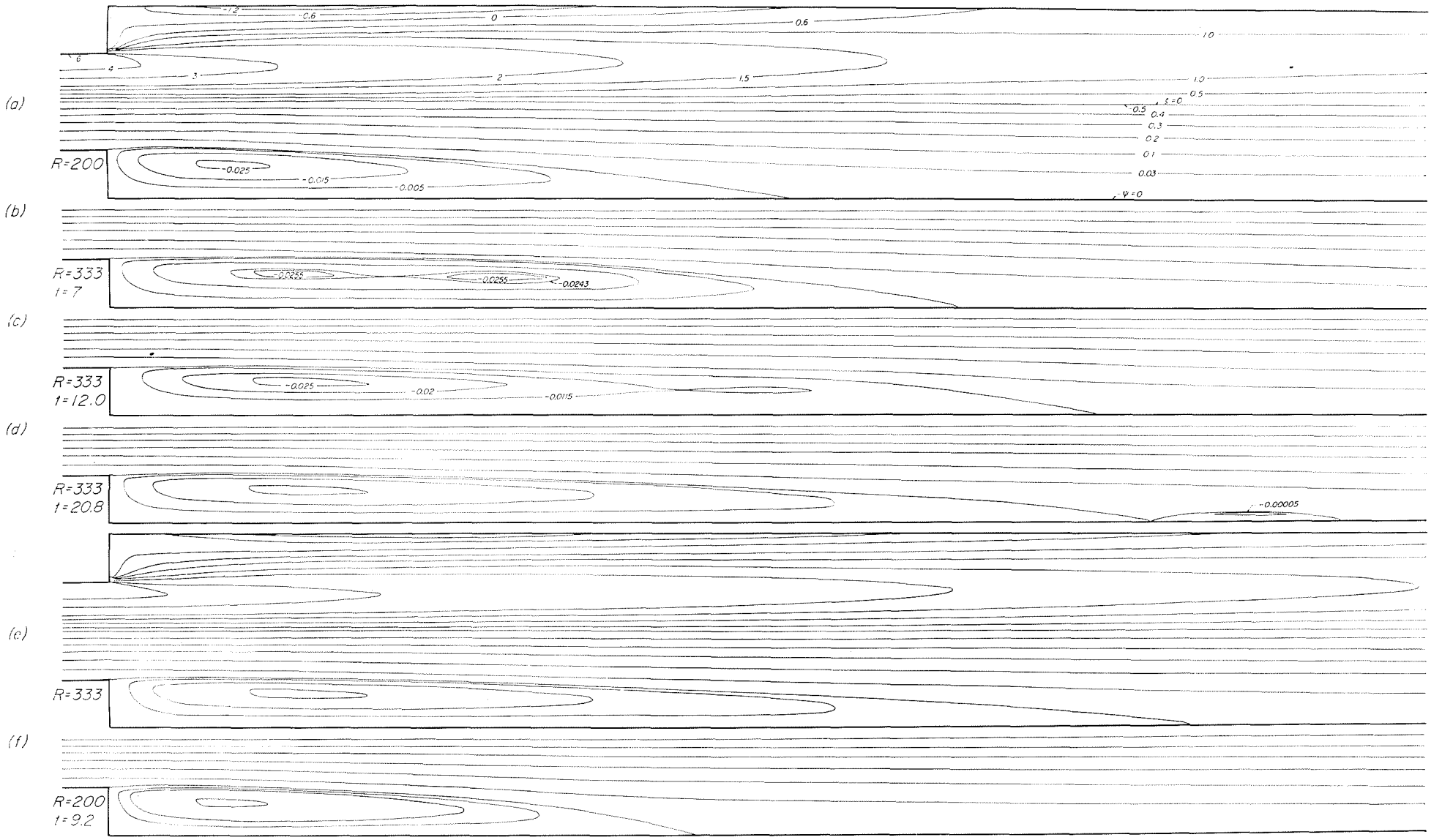

4/ Streamlines and vorticity contour lines for a variation of the Reynolds number from 200 to 333 (*a* to *e*). The diagram (*f*) shows the streamlines for the minimum size of the eddy when the Reynolds number is reduced back to 200.

Répartition des lignes de courant et des profils de vorticité, correspondant à une variation du nombre de Reynolds de 200 à 333 (a à e). *Le schéma* (f) *représente les lignes de courant correspondant aux dimensions minimales du tourbillon, le nombre de Reynolds étant ramené à 200.*

pattern for $\mathcal{R} = 333$ is shown as obtained from the flow pattern for $\mathcal{R} = 200$ by the device of changing the Reynolds number in the finite-difference equations from 200 to 333 while keeping the dimensionless rate of flow constant. The flow pattern for $\mathcal{R} = 200$ was obtained by "accelerating" from $\mathcal{R} = 48$ to $\mathcal{R} = 93.3$, and then from 93.3 to 200. But before doing this, a verification of the computational scheme for the unsteady approach was effected; the verification consisted of using the already known values of the stream and vorticity functions for $\mathcal{R} = 48$ obtained from the steady approach as initial values for a calculation using the unsteady approach for precisely $\mathcal{R} = 48$. The program was run for 120 time intervals without inducing any important variation in the flow pattern; the maximum local variation of the stream function was found to be such that $\delta\psi/\psi_0 < 0.0002$ was satisfied everywhere. The mesh size used was 1/16, based on the fact that calculations for $\mathcal{R} = 48$ gave practically the same result with 1/16 and 1/32. The calculations for an increase of the Reynolds number from 48 to 93.3 yielded a flow pattern that agreed very well with the one calculated with a finer mesh using the steady approach. For increments from 93.3 to 200 and from 200 to 333, no calculations are available via the steady approach, and one must rely on the confidence already developed by the above-mentioned verifications and by the results obtained by other investigators [1, 2, 3, 10]. The authors have verified experimentally the existence of rather long eddies in the case of axisymmetric flow [11]; however, in addition to the desirability of having a physical counterpart, there is the very valuable aspect of the power of the unsteady approach for calculations that would not be possible with explicit discretized equations without much finer meshes requiring much more computer storage. It is believed that still longer steps can be taken with this method in order to obtain flow at a given Reynolds number from the flow at a quite different number.

The successive diagrams of Figure 4, from (*a*) to (*e*), show the initial, intermediate, and final steps of the computational "flow" from $\mathcal{R} = 200$ to $\mathcal{R} = 333$. A notable feature of the eddy growth is that the flow within the eddy undergoes an evolution that seems realistic in the sense that breaking of the eddy in two is observable experimentally in long eddies; it is true that this happens under actual accelerative forces, but the type of acceleration imposed in this computational model is perhaps not as unnatural as it may appear at first glance. It should also be mentioned that the second eddy not only decays as the steady-state is approached but finally separates and is carried away. If it were possible to provide a certain amount of heat to the very slow motion of a liquid of low viscosity so that a rapid change in viscosity could happen everywhere without changing the rate of discharge, one would come quite close to the "experiment" performed in the computer by changing $\mathcal{R}$ from one value to another. The splitting of the eddy in two was also observed when changing the Reynolds number from 93.3 to 200 but not from 48 to 93.3. The authors have performed calculations [12] imposing a true acceleration upon their computational flow through an expansion and found that the breaking of the eddy in two happened again, in a manner similar to that shown in Figure 4.

The last diagram in this figure is also for $\mathcal{R} = 200$, but it has been obtained by reducing the Reynolds number abruptly from 333 to 200; only the minimum eddy size is shown, because the eddy shrinks quite regularly as if it remained self-similar without splitting in two.

To supplement the information provided by Figure 4, the variation of relative eddy length L/D_0, the position of the eddy center L_2/D_0, and the dimensionless intensity of the eddy ψ_1/ψ_0, defined as the ratio between absolute value of the stream function in the center of the eddy and the discharge, are given in Figures 5 and 6 for the computational growth of the eddy when the Reynolds number is varied from 48 to 93.3 and from 333 to 200, respectively. The length of the eddy shows in both cases a characteristic of highly damped oscillations in the fact that the eddy becomes either too long or too short once before reaching the final length. A similar behavior, in a more pronounced manner, is also exhibited by the ratio ψ_1/ψ_0; in this case the function pendulates twice before reaching equilibrium.

The relative length, L/D_0, of the eddy for the steady-state solution is shown in Figure 7 as a function of the Reynolds number. It can be seen that the relative length of the laminar eddies at a flow expansion is very nearly a linear function in the range $\mathcal{R} = 15$ to $\mathcal{R} = 100$; the line does not go through the origin, it actually curves up slightly to reach a value of 0.29 for $\mathcal{R} = 0$. The results of the unsteady-approach calculation fall close to the straight line determined by the steady-state calculations for intermediate values of the Reynolds number. The line for L_2/D_0 is also very nearly straight.

The continuous growth of the eddy size should not neccessarily imply a continuous increase in relative intensity of the eddy; one should rather expect that, when the laminar eddy became very long, a good portion of it would be represented by almost parallel flow and counterflow driven by the main stream and therefore should increase in the same ratio. The lines for ψ_1/ψ_0 and ζ_1/ζ_0 (Fig. 7) show that there is for these two quantities a definite trend toward a constant value; the first has been defined above; the second represents the absolute maximum boundary vorticity in the zone of back flow divided by the maximum vorticity of the upstream uniform flow.

Only qualitative experiments for two-dimensional flows were performed during this investigation; they confirmed the existence of long stable laminar eddies. Similar computations have been performed for expansions of axisymmetrical flow and they were verified experimentally in a quantitative manner [5]. A different verification, of indirect nature, for the calculations presented in this paper was based on integrating the results to obtain the velocity and pressure distributions [9]; these were then introduced in the Navier-Stokes equations, and the corresponding residues referred to U_0^2/D_0 for the x- and y-components were determined. The residues are represented by means of contours lines in Figure 8; they are small over most of the field, but near the entrant corner they show important local deviations that could only be reduced if more refin-

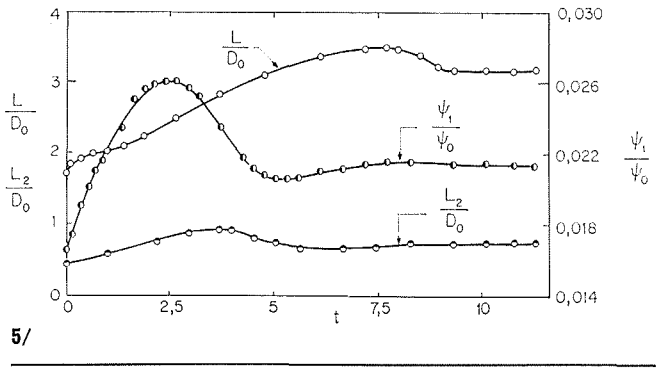

5/

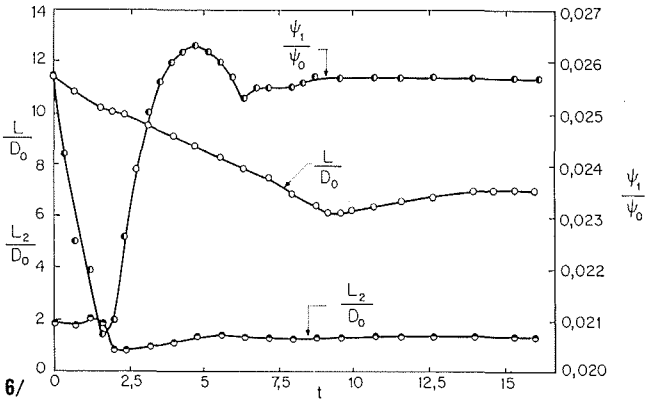

6/

5/ Unsteady approach. Reynolds number variation from 48 to 93.3. Eddy length L; location of the center of the Eddy L_2; intensity of the Eddy ψ_1.

Méthode non permanente. Variation du nombre de Reynolds de 48 à 93,3. L = longueur du tourbillon, L_2 désigne l'emplacement du centre du tourbillon et ψ_1 l'intensité du tourbillon.

6/ Unsteady approach. Reynolds number variation from 333 to 200. Eddy length, L; location of the center of the eddy, L_2. Intensity of the eddy, ψ_1.

Méthode non permanente. Variation du nombre de Reynolds de 333 à 200. L = longueur du tourbillon, L_2 désigne l'emplacement du centre du tourbillon et ψ_1 l'intensité du tourbillon.

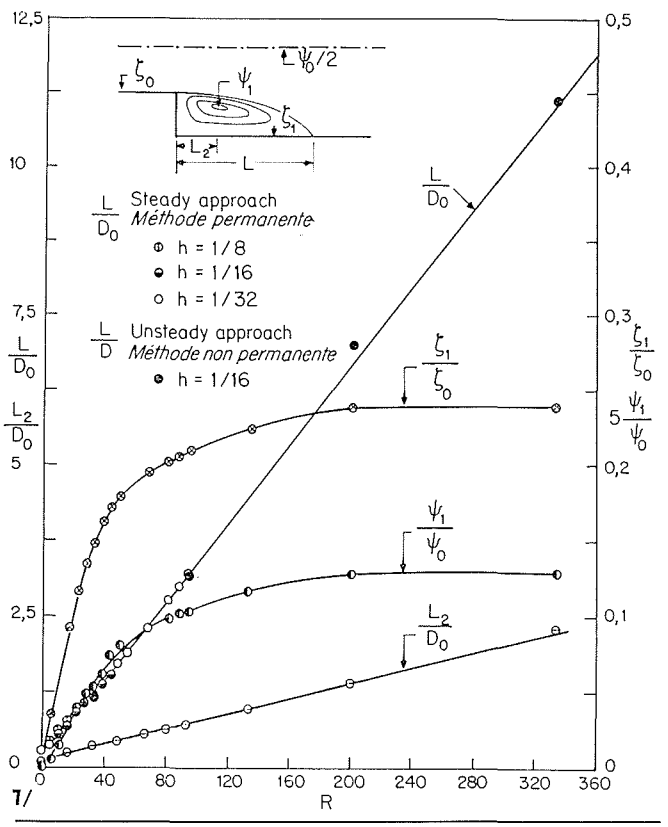

7/

7/ Two-dimensional conduit expansion of ratio 2 : 1 Steady flow. Eddy length L; location of eddy center L_2, intensity of the eddy ψ_1, highest vorticity in the zone of back flow ζ_1.

Agrandissement dans un rapport de 2 à 1 d'une conduite à deux dimensions. Régime d'écoulement permanent. L est la longueur du tourbillon, L_2 désigne l'emplacement du centre du tourbillon, Ψ_1 l'intensité du tourbillon et ζ_1 la vorticité maximale dans la zone des courants de retour.

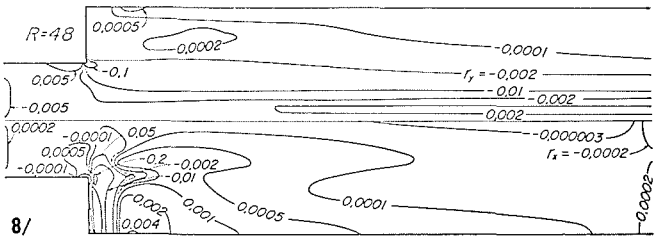

8/

8/ Residues, r_x, r_y, for the Navier-Stokes equations. The upper part is for the y-component, the lover part for the x-component.

Valeurs résiduelles, r_x, r_y, pour les équations de Navier-Stokes. La partie supérieure du schéma correspond à la composante en y et la partie supérieure à celle en x.

ed techniques requiring extra computer time were used. It is believed, however, that the improvement on the flow pattern would be a minor one, although the circulation of the pressure field would certainly be improved by a better computational treatment around the corner.

Conclusions

The use of discretized forms of the equations for viscous flow, when electronic computers of large capacity and high speed are available, provides a powerful means of investigating flows that cannot yet be studied by classical means of analytical integration. In this research work, the steady-flow zone of separation in a two-dimensional conduit expansion of ratio 2:1 was investigated by two different methods, i.e., the direct calculation of the steady-state solution using the equations without unsteady terms, and the asymptotical approach by means of the equations with unsteady terms. For the range of Reynolds numbers in which both methods were applied, a very good agreement was obtained. It was found that for high Reynolds numbers the unsteady approach was

much more stable than the steady approach for the same mesh size. Once the flow for a certain Reynolds number is known, the unsteady approach permits calculation of the flow for another quite different lower on higher Reynolds number.

Acknowledgments

Most of the foregoing investigation was supported by the Army Research Office, Durham, under Contract No. DA-ARO(D)-31-124-G174. Part of the computer time in the final phase of the work was financed by the Graduate College of the University of Iowa. The authors gratefully acknowledge the very valuable advice given by Mr. J. E. Fromm of Los Alamos Scientific Laboratory, University of California. The calculations were performed with the IBM 7044 computer at the University of Iowa Computer Center.

List of symbols

D_0 : spacing in the narrow part of the conduit;
L : length of eddy;
L_2 : distance between the eddy center and the expansion section;
$\mathcal{R}$: Reynolds number $U_0 D_0/\nu$;
U_0 : mean velocity in the narrow part of the conduit;
h_0 : mesh size;
h : dimensionless mesh size h_0/D_0;
p : dimensionless pressure;
t : dimensionless time;
u : dimensionless velocity component in the x-direction;
v : dimensionless velocity component in the y-direction;
x : dimensionless Cartesian abscissa;
y : dimensionless Cartesian ordinate;
ζ : dimensionless vorticity;
ν : kinematic viscosity;
ρ : mass density;
ψ : dimensionless stream function.

SUBSCRIPTS :
$_i$: index for x;
$_j$: index for y.

SUPERSCRIPTS :
^{k} : iteration index;
^{n} : time index.

Bibliography

[1] FROMM (J. E.). — A Method for Computing Nonsteady, Incompressible, Viscous Flow. *Los Alamos Scientific Laboratory, Report LA-2910* (1963).

[2] FROMM (J. E.) and HARLOW (F. H.). — Numerical Solution of the Problem of Vortex Street Development. *The Physics of Fluids* (July 1963).

[3] THOM (A.) and APELT (C. J.). — Field Computations in Engineering and Physics, *D. Van Nostrand*, London (1961).

[4] MACAGNO (E. O.). — Estudio experimental de corrientes planas con el aparato de Hele-Shaw. *Ciencia y Técnica*, vol. 114, No. 576 (1950).

[5] MACAGNO (E. O.). — Some New Aspects of Similarity in Hydraulics, Symposium on Dimensional Analysis, Similitude, Scalting and Modeling, University of Wisconsin (March 18-19, 1965).

[6] MACAGNO (E. O.) and HUNG (T. K.). — Computional Stability of Explicit-difference Form of Equations for Viscous Fluid Flow. (Submitted for publication.)

[7] WOODS (L. C.). — The Numerical Solution of 4th Order Differential Equations. *Aeronautical Quarterly*, vol. V (1954).

[8] MILNE (W. E.). — Numerical Solution of Differential Equations, *John Wiley and Sons*, New York (1953).

[9] MACAGNO (E. O.) and HUNG (T. K.). — Pressure, Bernoulli sum, and Momentum and Energy Relations in a Two-Dimensional Laminar Zone of Separation. (Submitted to the *Physics of Fluids* for publication.)

[10] PEARSON (C. E.). — A Computational Method for Viscous Flow Problems. *J. Fluid Mechanics*, vol. 21, part 4 (1965).

[11] MACAGNO (E. O.) and HUNG (T. K.). — Computation and experimental study of a captive annular eddy. (To be published.)

[12] MACAGNO (E. O.) and HUNG (T. K.). — Accelerated Flow in a Two-Dimensional Conduit Expansion. (To be published.)

Résumé

Les tourbillons laminaires dans un élargissement d'une conduite à deux dimensions

par T. K. Hung * et E. O. Macagno **

L'article expose les résultats de calculs effectués à l'aide d'un ordinateur électronique, intéressant la zone de décollement de l'écoulement dans un élargissement, dans un rapport de 2 à 1, d'une conduite à deux dimensions, et présente des schémas d'écoulement, et des profils de vorticité, correspondant à des nombres de Reynolds de 0 à 333. Deux méthodes ont été employées : dans l'une, on détermine directement le régime permanent à partir d'équations sans termes non permanents, et dans l'autre, on aborde la solution par un procédé asymptotique, correspondant à l'intégration numérique des

* Research Associate, Institute of Hydraulic Research, The University of Iowa, Iowa City, Iowa.

** Associate Professor, Department of Mechanics and Hydraulics; Research Engineer, Institute of Hydraulic Research, The University of Iowa, Iowa City, Iowa.

équations présentant des termes d'accélération localisée. A conditions égales, la méthode non permanente s'est révélée stable, au point de vue du calcul, alors que la méthode permanente devenait instable; lorsque les deux méthodes étaient stables, leurs résultats montraient une excellente concordance.

Les équations qui ont permis de construire le schéma des différences correspondant au modèle mathématique ayant servi pour la présente étude, sont les équations (7) et (8), couplées par l'intermédiaire des conditions aux limites. La substitution de l'équation (7) en (8) fournirait une seule équation du 4e ordre, mais l'expérience du passé a démontré la grande difficulté du traitement numérique d'une telle équation.

L'étude de l'écoulement à travers l'élargissement de la conduite s'est faite par deux méthodes. L'une, que nous appellerons la méthode « permanente », a consisté à calculer la solution en régime permanent, à partir de l'équation (8), et sans intervention du terme non permanent ζ_t; l'autre méthode, que nous appellerons la méthode « non permanente », était basée sur l'application de l'équation (8) « telle quelle » à l'une des solutions déjà fournies par la méthode permanente. La méthode non permanente a permis le passage, sans modification des dimensions de la maille, de l'écoulement correspondant à un nombre de Reynolds donné, à un autre écoulement, correspondant à un nombre de Reynolds bien plus élevé (ou plus faible). Les équations aux différences finies intervenant dans la méthode permanente sont les équations (9) et (10), obtenues à partir des équations (7) et (8) à l'aide de formules du genre des (11) et (12). Dans les équations aux différences finies (9) et (10), l'indice k indique le nombre des itérations; celles-ci se font dans le sens des j et des i croissants, ou bien, ce qui revient au même, des y et des x croissants.

Pour la méthode non permanente, on a employé les équations (13) et (14), dans lesquelles n représente l'indice du temps. On notera que la première de ces deux équations indique la possibilité de calculer ζ à l'instant $(n + 1)\,\delta t$, à partir des valeurs stables de ψ et de ζ à l'instant $n\delta t$, et celle de ζ à l'instant $(n - 1)\,\delta t$. Une fois faits les calculs de ζ à l'instant $(n + 1)\,\delta t$, on calcule la fonction de courant par itération, à l'aide de l'équation (14).

Etant donné qu'il semblait si évident que les solutions correspondant au régime permanent s'obtiendraient plus aisément à partir d'équations sans termes non permanents, la première partie de la présente étude a été consacrée à l'intégration des équations (9) et (10) en partant du cas-limite de la disparition des forces d'inertie, soit du cas bien connu de l'écoulement de fluage. Ensuite, une fois déterminé l'écoulement correspondant à un nombre de Reynolds donné, on a fait augmenter la valeur de ce nombre dans l'équation (10), et on a repris le calcul autant de fois qu'il fallait pour obtenir des valeurs bien établies. A cause d'instabilités du calcul, il n'est possible, pour des dimensions de maille données, de poursuivre ce procédé, et d'obtenir de bons résultats, que jusqu'à un certain nombre de Reynolds; une fois ce nombre de Reynolds atteint, le passage à une maille de plus petites dimensions s'impose.

L'influence des dimensions de maille, et des méthodes de balayage, sur la stabilité des calculs, a été étudiée à l'aide d'un écoulement uniforme et perturbé, en faisant pour ce dernier des calculs correspondant à une partie de la conduite à deux dimensions. Les équations (15) à (21) représentent la méthode par laquelle les auteurs ont abordé les conditions aux limites.

Dans toute expérience réelle ayant pour objet la détermination d'une zone de décollement, il est nécessaire d'accélérer le fluide progressivement, à partir de son état initial au repos. Autrement dit, on n'envisagerait guère d'établir l'écoulement permanent recherché d'un seul coup. Par conséquent, il semble qu'un schéma de calcul plus naturel, pour la détermination de la zone de décollement, devrait, en principe, être propre à reproduire, sur le modèle mathématique, ce qui se passe dans le milieu physique. Cependant, ceci n'a été fait qu'après s'être heurté à des difficultés insurmontables avec la méthode permanente, qui de prime abord était censée plus simple et rapide. Or, la méthode non permanente s'est montrée à la fois d'un maniement tout aussi aisé que la méthode permanente, et beaucoup plus stable. La méthode permanente représentait un moyen différent de déterminer des schémas d'écoulement; elle servait également à vérifier et à guider la méthode non permanente, dont on préconisera néanmoins l'emploi pour toute nouvelle étude. Le procédé employé a consisté à changer le nombre de Reynolds dans l'équation (13), sans modifier les valeurs de la fonction de courant aux limites, ce qui peut se concevoir comme une modification brusque de la viscosité, la valeur du débit restant constante.

Les figures 2 et 3 représentent une série de schémas d'écoulement, et les profils de vorticité correspondants, obtenus par la méthode permanente. Ces figures ne correspondent qu'à une partie des calculs exécutés pour la gamme des nombres de Reynolds s'échelonnant de 0 jusqu'à presque 100. Les résultats des calculs effectués à l'aide de la méthode non permanente sont représentés sur la figure 4, qui montre le schéma d'écoulement correspondant à $\mathcal{R} = 333$, et ayant été obtenu à partir de celui correspondant à $\mathcal{R} = 200$ par un artifice consistant à changer le nombre de Reynolds dans les équations aux différences finies de 200 à 333, tout en maintenant constante la valeur du débit sans dimensions. Le schéma d'écoulement correspondant à $\mathcal{R} = 200$ a été obtenu en « accélérant » de $\mathcal{R} = 48$ à $\mathcal{R} = 93{,}3$, et ensuite de $\mathcal{R} = 93{,}3$ à $\mathcal{R} = 200$. Les schémas (*a*) à (*e*) de la figure 4 montrent, successivement, les étapes initiale, intermédiaire, et finale de « l'écoulement » du calcul, en passant de $\mathcal{R} = 200$ à $\mathcal{R} = 333$. Une caractéristique intéressante de la croissance du tourbillon est que l'écoulement en son intérieur évolue d'une manière qui paraît réaliste, en ce sens que l'observation expérimentale de la scission du tourbillon en deux parties est possible, dans le cas des tourbillons de forme allongée. Des calculs imposant une accélération réelle du débit « modèle » par un élargissement, ont déjà été effectués sous la direction du deuxième auteur de l'étude; il s'est montré que, là aussi, le tourbillon se scindait en deux parties, de manière semblable à celle indiquée sur la figure 4. Le dernier schéma de cette figure correspond également à $\mathcal{R} = 200$, mais il a été obtenu en réduisant brutalement le nombre de Reynolds de 333 à 200; seul y figure le tourbillon de plus petites dimensions, puisque le tourbillon se rétrécit tout à fait régulièrement, comme s'il restait semblable à lui-même, sans se scindre en deux.

Les figures 5 et 6 indiquent la croissance calculée de la longueur relative du tourbillon, la position du centre du tourbillon, et son intensité, due aux variations du nombre de Reynolds, respectivement de 48 à 93,3, et de 333 à 200. La figure 7 présente quatre caractéristiques de tourbillons permanents, en fonction du nombre de Reynolds; on y notera avec intérêt la croissance linéaire de la longueur du tourbillon.

L'utilisation de formes discrétisées des équations correspondant à l'écoulement visqueux, lorsque l'on dispose d'ordinateurs à grande capacité et rapidité de calcul poussée, met à disposition un puissant moyen pour l'étude des écoulements résistant encore aux procédés classiques d'intégration analytique. Un des avantages des modèles mathématiques est qu'ils permettent d'emmagasiner « l'écoulement », et « d'effectuer des observations complémentaires » à n'importe quel moment par la suite. C'est exactement ce qu'ont fait les auteurs, en calculant la pression, la somme de Bernoulli, les efforts normaux et tangentiels, les termes tenant compte de la qualité de mouvement et de l'impulsion, et les équations de l'énergie et du travail, correspondant à l'un des écoulements emmagasinés dans les élargissements de conduites. Les résultats de ces « observations » ont déjà été présentés en vue de leur publication.